Available online at www.sciencedirect.com
SCIENCE DIRECT®
International Journal of Mass Spectrometry 228 (2003) 429–437
International Journal of Mass Spectrometry
www.elsevier.com/locate/ijms

Two-center three-electron bonds involving selenium

Joseph E. King, Andreas J. Illies*

Department of Chemistry, 179 New Chemistry Building, Auburn University, Auburn, AL 36849-5312, USA

Received 25 November 2002; accepted 18 March 2003

Abstract

We report the first known experimental gas-phase study of two-center three-electron bonding involving selenium. Ions studied include: $[(CH_3)_2Se\therefore Se(CH_3)_2]^+$, $[(CH_3)_2Se\therefore Se(CH_3)_2]^+$ and $[(CH_3)_2Se\therefore ICH_3]^+$. We investigated these ions using metastable and collision-induced dissociation MS/MS methods. The metastable spectra of $[(CH_3)_2Se\therefore Se(CH_3)_2]^+$, $[(CH_3)_2Se\therefore S(CH_3)_2]^+$ and $[(CH_3)_2Se\therefore ICH_3]^+$ show direct cleavage of the Se ∴ Se, Se ∴ S and Se ∴ I bonds. In addition, the metastable spectrum of $[(CH_3)_2Se\therefore ICH_3]^+$ shows fragmentation via a rearrangement path with ejection of the iodine atom. These metastable and collision-induced dissociation spectra are all consistent with Se ∴ Se, Se ∴ S and Se ∴ I hypervalent interactions. Spectra of $[(CH_3)_2Se\therefore (CH_3)_2]^+$ were also compared with spectra of $[CH_3Se–SeCH_3]^{\bullet+}$, these comparisons also very strongly support the two-center three-electron Se ∴ Se interaction in $[(CH_3)_2Se\therefore Se(CH_3)_2]^+$. Experimental equilibrium studies of $(CH_3)_2Se^{\bullet+} + Se(CH_3)_2 \rightleftharpoons [(CH_3)_2Se\therefore Se(CH_3)_2]^+$ resulted in $\Delta H^\circ_{rxn} = -95 \pm 3$ kJ/mol and $\Delta S^\circ_{rxn} = -76 \pm 6$ J/mol K. Since in this reaction, $\Delta H^\circ_{rxn} = -\Delta H^\circ_{bond}$, the experiment yields a bond enthalpy of 95 kJ/mol at 511 K. We believe that these are the first gas-phase experiments on 2c-3e bonding involving selenium and thus, this may be the first experimental determination of a Se ∴ Se bond enthalpy.

Keywords: Selenium; Bonding; Equilibrium; MS/MS

1. Introduction

Much research has been devoted to studies of two-center three-electron (2c-3e) bonds in both the gas phase and solution. These hypervalent interactions, first described by Linus Pauling in 1931 relate to both reactive intermediates and stable products [1]. Our interest in 2c-3e interactions stems mostly from a desire to understand the fundamentals of these interactions. We have published gas-phase reports on S ∴ S, X ∴ X, X ∴ Y and S ∴ X, where X and Y represent the halogens F, Cl, Br and I [2–10]. Other groups, namely Nibbering and coworkers' [11] and Baer and coworkers' [12] groups, have also published experimental gas-phase results on 2c-3e bonds. Asmus [13] has been the main player in studies of these bonds in solution.

Though much research has been devoted to studies on 2c-3e bonding interactions, reports on gas-phase interactions involve just a few atoms. In this article, we report what we believe are the first gas-phase studies on 2c-3e bonding involving selenium atoms. Asmus [13] has reported UV-Vis absorptions, which he has attributed to Se ∴ Se interactions in solution. A Se ∴ Se interaction has also been reported in an ESR

* Corresponding author. Tel.: +1-334-844-6968; fax: +1-334-844-6959.
E-mail addresses: kingje1@auburn.edu (J.E. King), illieaj@auburn.edu (A.J. Illies).

1387-3806/$ – see front matter © 2003 Elsevier Science B.V. All rights reserved.
doi:10.1016/S1387-3806(03)00136-2

solid-state study [14] while such interactions have also been computationally explored [15].

Selenium is an essential element for life as a micronutrient [16]. Selenium is found as a selenocysteine residue and as a component of a cofactor. As selenocysteine, selenium has been shown to be essential for catalytic activity in mammalian thioredoxin reductase. Selenium also is present in our atmosphere; however, its lifetime there is not very long [17]. We hope that this research will lead to a better understanding of 2c-3e bonding in general and to a more complete understanding of how selenium may interact in this manner.

2. Experimental

Experiments were carried out using two mass spectrometers. MS/MS experiments were carried out on a modified ZAB-1F. This instrument was modified by addition of a collision cell in the second field-free region, by placing the electron multiplier on-axis to reduce discrimination in the MIKES scan and by a home-built ion source. These modifications have been described [3]; however, a brief description of the ion source is warranted. The ion source, built from a large oxygen-free copper block, is optimized for high-pressure and variable-temperature operation. The source has co-axial electron beam and ion-exit geometry and utilizes an ion extraction potential between the front plate and the rear plate. The inside source cross-section is large, resulting in a uniform ion extraction electric field drop within the source. Ions generated at the electron entrance drift through the 1-cm drift length to the ion exit slit; hence, they undergo numerous reactive collisions. The experiments described here were carried out around 315 K; we estimate that the ion source pressures were approximately 0.3–0.5 Torr. Kinetic energy release distributions (KERDs), were obtained by standard methods from metastable peak shape analysis [18]. CID spectra were recorded using helium as the stationary gas at pressures needed to reduce the main beam intensity by 40%.

Thermodynamic measurements were carried out using a DuPont 491 fitted with a high-pressure, variable-temperature ion source that resembles a miniature drift tube [3,4,19]. This source also has a co-axial electron entrance/ion exit geometry and contains four internal drift guard rings, which shape the electric drift field. Experiments on the equilibrium forming $[(CH_3)_2Se \therefore Se(CH_3)_2]^+$ were carried out with 0.010–0.032 Torr $Se(CH_3)_2$ in research grade CO_2. The total source pressure ranged from 0.5 to 0.8 Torr; higher ion source pressures resulted in collision-induced dissociation in the ion acceleration region and hence incorrect measurements of adduct ion intensities, while at lower ion source pressures equilibrium was not established. The ion source pressures in this instrument were directly measured with a MKS type 270B capacitance manometer. The source temperature ranged from 462 to 560 K and was measured with a platinum resistance element imbedded in the ion source copper wall. This ion source was designed and built with special attention for a uniform temperature, especially at the ion source exit. Towards this end, the ion exit slit is placed inside the massive copper block; this provides excellent heat transfer and eliminates a temperature gradient at the exit slit. Both continuous and pulsed experiments were conducted.

In all experiments, the association adducts were formed by introducing gas samples into the ion source and forming the ions of interest by ion–molecule reactions. In every case, spectra of only the ^{80}Se isotopes were examined. In the metastable and CID experiments, some artifact peaks from other isotopes were observed; however, these artifact peaks were easily identified. In the thermodynamic experiments, quantitative measurements of only the ^{80}Se isotope were made, however, those measurements were corrected by the natural abundances of all the isotopes to reflect the entire ion intensity.

All chemicals were used as purchased. CO_2 was purchased from MG Industries, $Se_2(CH_3)_2$ from Strem and CH_3I, $S(CH_3)_2$ and $Se(CH_3)_2$ from Aldrich. Due to the toxicity of selenium compounds, great care was taken to properly vent all vacuum pumps used into hoods.

All chemicals used were commercially available. Sample preparation was accomplished by simple outgassing through several freeze-pump-thaw cycles with a Pyrex vacuum line with a base pressure of approximately 5×10^{-3} Torr.

3. Results and discussion

3.1. MS/MS experiments

3.1.1. $[(CH_3)_2Se \therefore Se(CH_3)_2]^+$

Metastable and CID experiment were carried out on all three ions listed in the abstract. The metastable fragmentation of $[(CH_3)_2Se \therefore Se(CH_3)_2]^+$ (shown in Fig. 1) results in a single fragmentation path. The larger peak at *m*/*z* 110 corresponds to fragmentation of $[(CH_3)_2{}^{80}Se \therefore {}^{80}Se(CH_3)_2]^+$ while the smaller peaks at *m*/*z* 108 and 112 correspond to fragmentation of $[(CH_3)_2{}^{78}Se \therefore {}^{82}Se(CH_3)_2]^+$. For this fragmentation, the charge is retained equally on either isotopic moiety, resulting in the two satellite peaks. The kinetic energy release distribution (KERD) for this process was measured and yielded an average kinetic energy release (aKER) of 27 meV. Small aKERs are indicative of reactions with very small or no reverse activation barriers. Direct cleavage of bonds is a class of reactions which falls into this category. The observed aKER of 27 meV is consistent with many we have observed for direct cleavage on other studies of 2c-3e bonded systems. We suggest that the observed aKER implies direct cleavage of a bond involving the Se on the $(CH_3)_2Se^{\bullet+}$ fragment.

The metastable spectrum for $[CH_3Se–SeCH_3]^{\bullet+}$ from direct ionization of $CH_3Se–SeCH_3$ is shown in Fig. 2 for comparison purposes. This spectrum is very different from that for $[(CH_3)_2Se \therefore Se(CH_3)_2]^+$. The main peak in the spectrum is at *m*/*z* 109. This ion at *m*/*z* 109 cannot come from simple direct cleavage of a bond; rather it must arise from a rearrangement mechanism resulting in $C_2H_5Se^+$ and neutral $SeH^{\bullet}$. The aKER for this fragmentation is 61 meV. Although this is not large, it is about double that for the direct fragmentation above. Larger KERs are usually observed for reactions involving rearrangements and reverse activation barriers. Thus, this average 61 meV release supports a rearrangement relative to the 27 meV release observed for direct fragmentation of $[(CH_3)_2Se \therefore Se(CH_3)_2]^+$. The metastable spectra of $[(CH_3)_2Se \therefore Se(CH_3)_2]^+$ and $[CH_3Se–SeCH_3]^{\bullet+}$ each only have one major product peak; however, the mechanisms giving rise to the products are very different. The mechanism for the former involves direct cleavage of a bond while the mechanism for the latter involves rearrangement followed by bond cleavage.

The CID spectrum of $[(CH_3)_2Se \therefore Se(CH_3)_2]^+$ is shown in Fig. 3. The most intense peak for $[(CH_3)_2Se \therefore Se(CH_3)_2]^+$ is the direct cleavage of the $Se \therefore Se$ bond yielding $(CH_3)_2Se^{\bullet+}$. This fragmentation reaction is the same as that in the metastable

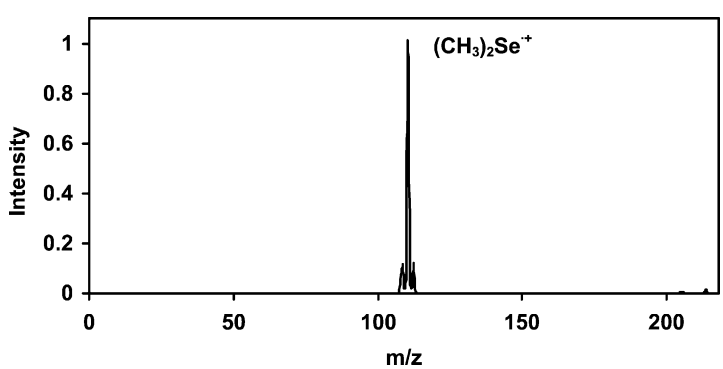

Fig. 1. The metastable spectrum of $[(CH_3)_2Se \therefore Se(CH_3)_2]^+$ showing direct cleavage of the 2c-3e bond yielding *m*/*z* 110 $(CH_3)_2Se^+$. The smaller peaks are due to the same chemical cleavage from ions containing $^{78}Se^{82}Se$.

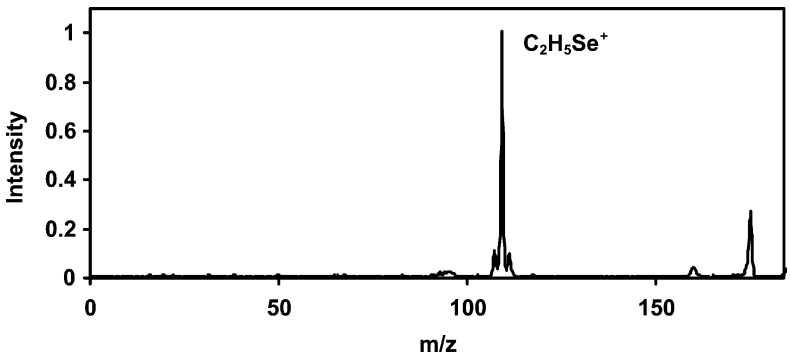

Fig. 2. The metastable spectrum of $[CH_3Se–SeCH_3]^{\bullet+}$. The larger peak at *m/z* 109 is that for a rearrangement reaction yielding $C_2H_5Se^+$. The smaller peaks are due to CID that could not be reduced due to the very weak metastable product intensity.

spectrum. It is interesting to note that peaks for loss of one, two, three and four methyl groups corresponding to $(CH_3)_3Se_2^+$, $(CH_3)_2Se_2^{\bullet+}$, $CH_3Se_2^+$, $Se_2^{\bullet+}$ are observed. In addition, a peak corresponding to one methyl loss from $(CH_3)_2Se^{\bullet+}$ is observed. Hence, the CID spectrum contains peaks for almost every possible methyl loss. This suggests a relatively large cross-section for Se–C bond cleavage by CID. The strong peak at *m/z* 110 for $(CH_3)_2Se^{\bullet+}$ and the peak at *m/z* 160 for $Se_2^{\bullet+}$ support our hypothesis that the parent ion contains a Se∴Se connectivity.

The CID spectrum for $[CH_3Se–SeCH_3]^{\bullet+}$ is shown in Fig. 4. This spectrum differs from that in Fig. 3 in that the product ion CH_3Se^+ resulting from direct Se–Se cleavage is not very intense; rather the most intense peak in the spectrum is that for loss of methyl from the parent ion. The fact that direct cleavage of the Se–Se bond is much less intense in $[CH_3Se–SeCH_3]^{\bullet+}$ relative to that for direct cleavage of the Se∴Se bond in $[(CH_3)_2Se∴Se(CH_3)_2]^+$ indicates that the 2c-2e bond is much stronger than the proposed 2c-3e bond in $[(CH_3)_2Se∴Se(CH_3)_2]^+$. We note that the only peak observed in the metastable spectrum, that requiring a rearrangement yielding $C_2H_5Se^+$ and $SeH^{\bullet}$ (Fig. 2), is much weaker in this CID spectrum. This is consistent with CID occurring on a shorter time frame where direct processes dominate.

The main findings from these metastable and CID spectra for $[(CH_3)_2Se∴Se(CH_3)_2]^+$ and $[CH_3Se–SeCH_3]^{\bullet+}$ parallel the main findings of earlier published results [3,4,6,10] on the metastable spectra

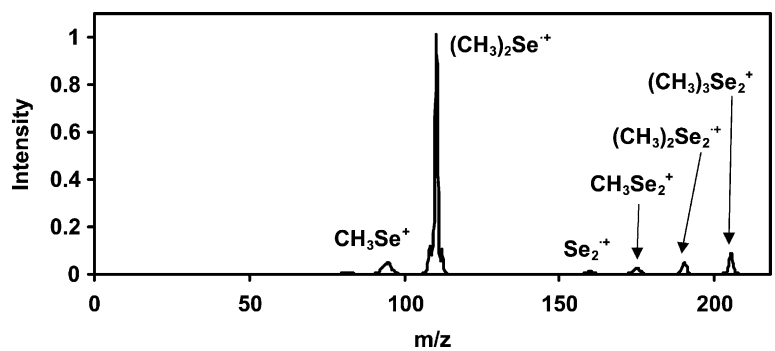

Fig. 3. The CID spectrum of $[(CH_3)_2Se∴Se(CH_3)_2]^+$. The most intense peak at *m/z* 110 $(CH_3)_2Se^{\bullet+}$ is due to cleaving the Se∴Se bond. Note that all possible ions due to methyl loss appear.

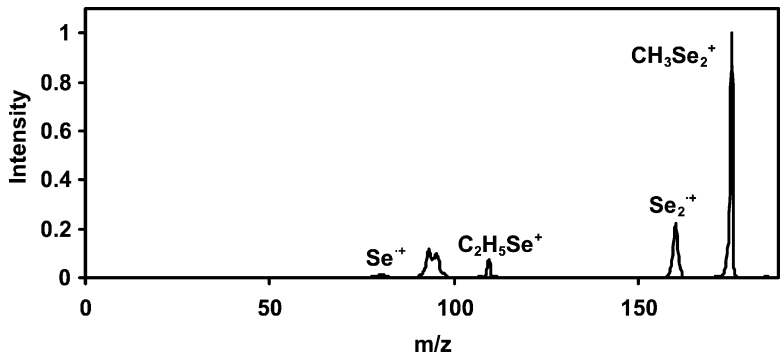

Fig. 4. CID spectrum of $[CH_3Se–SeCH_3]^{\bullet+}$. This spectrum shows a very weak peak for *m*/*z* 95 that results from cleaving the Se∴Se bond. All possible methyl losses appear.

for $[(CH_3)_2S \therefore S(CH_3)_2]^+$ and $[CH_3S–SCH_3]^{\bullet+}$ and very strongly suggest an entirely different bonding scheme for the two ions. These data support a 2c-2e bond in $[CH_3Se–SeCH_3]^{\bullet+}$ and a 2c-3e bond in $[(CH_3)_2Se \therefore Se(CH_3)_2]^+$. This is especially true of the large peak for $(CH_3)_2Se^{\bullet+}$ along with a weak peak for $Se_2^{\bullet+}$ in the CID spectrum of $[(CH_3)_2Se \therefore Se(CH_3)_2]^+$. We note the propensity for $CH_3^{\bullet}$ loss when the methyl group is directly bonded to Se is observed in these spectra.

3.1.2. $[(CH_3)_2Se \therefore S(CH_3)_2]^+$

The metastable and CID spectra of $[(CH_3)_2Se \therefore S(CH_3)_2]^+$ are straightforward and are not shown. The metastable spectrum shows one peak at *m*/*z* 110 $(CH_3)_2Se^{\bullet+}$ with a relatively small aKER around 23 meV. Surprisingly, the CID spectrum has only one intense peak also corresponding to $(CH_3)_2Se^{\bullet+}$. The spectrum however has weak peaks corresponding to most possible methyl losses. These metastable and CID results indicate a straightforward structure with Se∴S connectivity.

3.1.3. $[(CH_3)_2Se \therefore ICH_3)]^+$

The metastable spectrum of $[(CH_3)_2Se \therefore ICH_3]^+$ shown in Fig. 5 has two peaks, $(CH_3)_2Se^{\bullet+}$ at *m*/*z* 110 from direct cleavage of the Se∴I bond and a second peak at $m/z = 125$ which corresponds to $(CH_3)_3Se^+$. The first peak at *m*/*z* 110 results from a direct fragmentation of the parent ion with the charge residing on the fragment moiety with the lowest ionization potential and results in a relatively small aKER of 10 meV. The

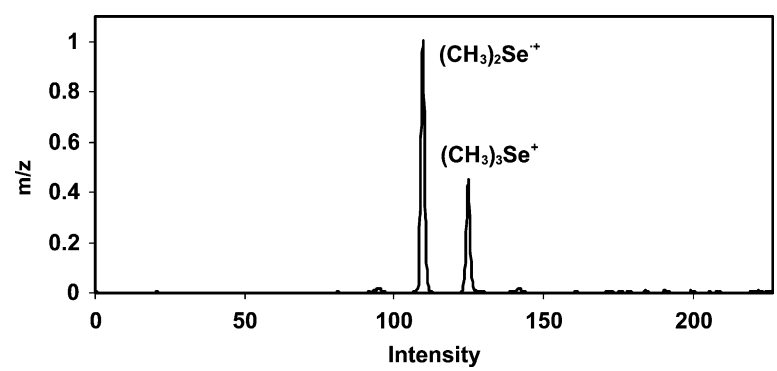

Fig. 5. The metastable spectrum of $[(CH_3)_2Se \therefore ICH_3]^+$. The spectrum shows the two competing fragmentation paths, direct fragmentation and rearrangement followed by fragmentation.

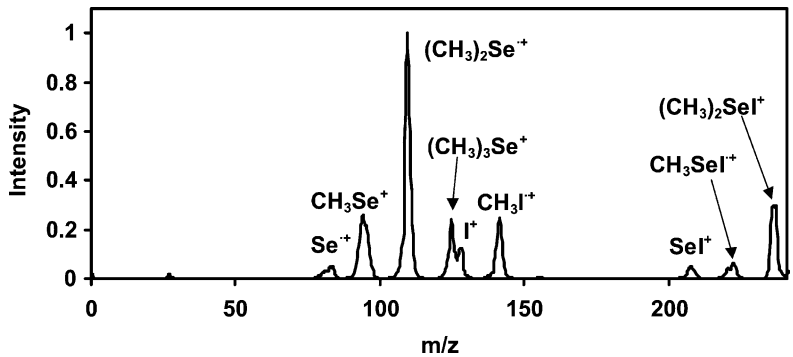

Fig. 6. The CID spectrum of $[(CH_3)_2Se\therefore ICH_3]^+$. The strongest product peak is *m/z* 110 $(CH_3)_2Se^{\bullet+}$. Again, this spectrum demonstrates product peaks for every possible methyl loss.

second peak, $(CH_3)_3Se^+$, corresponds to ejection of an iodine atom from the parent $[(CH_3)_2Se\therefore ICH_3]^+$ ion. This fragmentation requires a skeletal rearrangement and results in a larger aKER. This iodine ejection is similar to that observed in the metastable spectrum of $[(CH_3)_2S\therefore ICH_3]^+$.

The CID spectrum of $[(CH_3)_2Se\therefore ICH_3]^+$ is very rich in detail and is shown in Fig. 6. The largest peak is that for $(CH_3)_2Se^{\bullet+}$; however, all possible combinations of methyl loss from $[(CH_3)_2Se\therefore ICH_3]^+$ are observed. The peak for the rearrangement path yielding $(CH_3)_3Se^+$ at *m/z* 125 is also observed. This spectrum is in clear support of the proposed bonding. The very strong peak at *m/z* 110 for $(CH_3)_2Se^{\bullet+}$, the much weaker peak at *m/z* 142 for $CH_3I^{\bullet+}$ and the very weak peak at 207 for SeI^+ all implicate the $[(CH_3)_2Se\therefore ICH_3]^+$ connectivity.

3.2. Summary of the metastable and CID results

The metastable and CID spectra of $[(CH_3)_2Se\therefore Se(CH_3)_2]^+$, $[(CH_3)_2Se\therefore S(CH_3)_2]^+$ and $[(CH_3)_2Se\therefore ICH_3]^+$ all support the proposed structures. The spectra of $[(CH_3)_2Se\therefore Se(CH_3)_2]^+$ are compared to those of $[CH_3Se–SeCH_3]^{\bullet+}$. These comparisons are in very strong support of the 2c-3e bond in the former and a 2c-2e bond in the latter. The CID spectra of all three 2c-3e bonded adducts show peaks for almost every possible combination of methyl loss. The peaks corresponding to all methyl losses in the CID spectrum of $[(CH_3)_2Se\therefore S(CH_3)_2]^+$ (not shown) are much weaker relative to the methyl loss peaks in $[(CH_3)_2Se\therefore Se(CH_3)_2]^+$ and $[(CH_3)_2Se\therefore ICH_3]^+$. We do not have a firm explanation for this, however, we note that the less intense peaks are observed for the sulfur-containing cation. Sulfur, being in the third row of the periodic table is the smallest and "hardest" of the heteroatoms involved in our study. This may imply that loss of methyl groups attached to large soft atoms is much more facile than methyl loss from the smaller heteroatoms. However, the entire answer is probably more complex since $[(CH_3)_2Se\therefore S(CH_3)_2]^+$ should have two methyl groups attached to selenium and losses of those peaks does not appear to be intense.

3.3. Thermochemical equilibrium experiments

This study provided us the opportunity to attempt the first quantitative measurements of gas phase selenium–selenium 2c-3e bonding interactions. Equilibrium experiments on the reaction

$$(CH_3)_2Se^{\bullet+} + Se(CH_3)_2 \rightleftharpoons [(CH_3)_2Se\therefore Se(CH_3)_2]^+ \quad (1)$$

carried out as a function of temperature in CO_2 bath gas yield ΔH°_{rxn} and ΔS°_{rxn} from the van't Hoff equation

$$\ln K_{rxn} = -\frac{\Delta H^\circ_{rxn}}{RT} + \frac{\Delta S^\circ_{rxn}}{R}.$$

In order to collect meaningful equilibrium data, it is necessary to prove that the experiments measure true equilibrium constants. We routinely carry out four tests to demonstrate that equilibrium has been achieved: (1) We measure the equilibrium quotient as a function of the ion source extraction potential. These measurements are made with extraction potentials as low as feasible. (2) At a given temperature we measure the equilibrium quotient as a function of the neutral reagent gas pressure, in this case the $Se(CH_3)_2$ pressure. (3) We measure the equilibrium quotient as a function of the total ion source pressure by varying the bath gas pressure. (4) We measure the ion source residence time distributions to demonstrate constant ion current–time profiles. These measurements, the resulting van't Hoff plot and the bonding thermochemistry are presented here.

Measurements of the reaction quotient as a function of the ion extraction voltage were found to be constant at low voltages and to curve downwards at higher voltages. This downward curvature at higher voltages indicates that, in the region where the curvature takes place, equilibrium is not established, and the reactant ion intensity which appears in the denominator is larger than the equilibrium value. Thus, equilibrium has not yet been achieved at the higher extraction voltages which result in shorter ion residence times. We therefore averaged our measured equilibrium values at the low ion extraction voltages in the region with constant equilibrium quotient.

Naturally, the reaction quotient will be constant as the composition is changed. In these experiments, we were able to achieve equilibrium from 0.01 to 0.03 Torr of $(CH_3)_2Se$. Larger $(CH_3)_2Se$ pressures shifted the equilibrium too far to the right and made measurements of the $(CH_3)_2Se^{\bullet+}$ intensity very difficult. The total ion source pressure was also varied up to about 0.65 Torr. At higher pressures, collision-induced dissociation outside the ion source in the ion acceleration region resulted in a reduction of the association product ion intensity, $[(CH_3)_2Se \therefore Se(CH_3)_2]^+$.

The final test for equilibrium comes in the form of residence time distributions. When equilibrium is attained, residence times for both the product and reactant ions become identical. This is demonstrated in Fig. 7. This figure shows two superimposed RTDs; that for $(CH_3)_2Se^{\bullet+}$ is given by the dots while that for $[(CH_3)_2Se \therefore S(CH_3)_2]^+$ is given by the solid connected points. The figure clearly demonstrates that these two distributions are superimposable. In addition, the mathematical averages of these distributions are the same. We have found that identical RTDs represent a rigorous test of equilibrium.

With demonstrated equilibrium, data for a van't Hoff plot were collected. These data covered a range of conditions at each temperature. The results of

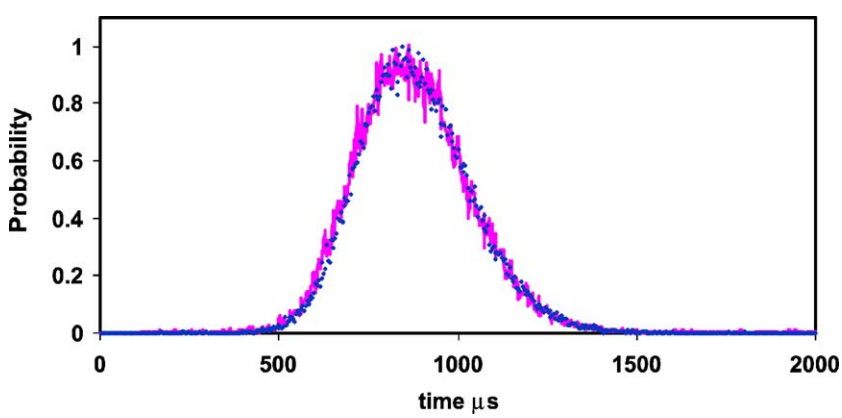

Fig. 7. Residence time distributions of $[(CH_3)_2Se]^{\bullet+}$ (dots) and $[(CH_3)_2Se \therefore Se(CH_3)_2]^+$ (connected points). The identical distributions show attainment of equilibrium in reaction (1).

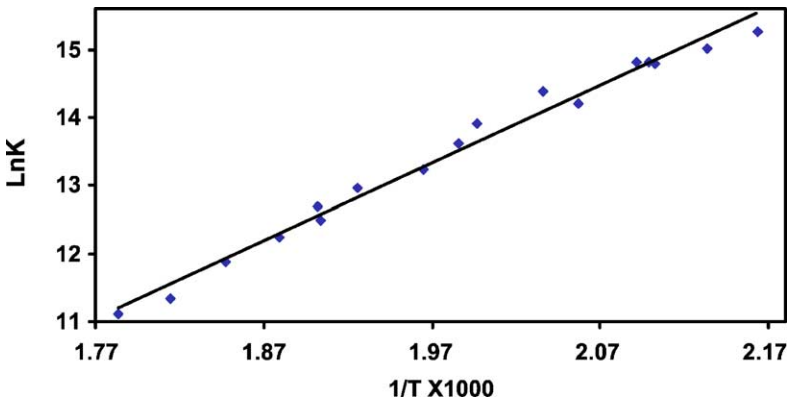

Fig. 8. The van't Hoff plot resulting from the equilibrium experiments on reaction (1).

the temperature studies are shown in Fig. 8. These data cover the entire measurable temperature range from 462 to 560 K [20]. The slope of this plot yields $\Delta H^{\circ}_{\mathrm{rxn}} = -95 \pm 3$ kJ/mol while the intercept yields $\Delta S^{\circ}_{\mathrm{rxn}} = -76 \pm 6$ J/mol K. These results are in excellent accord with similar reactions and chemical intuition. The bonding enthalpy is given by:

$$\Delta H^{\circ}_{\mathrm{bond}} = -\Delta H^{\circ}_{\mathrm{rxn}} = 95\,\mathrm{kJ/mol}$$

This value is about 50% of the mean diselenide RSe–SeR bond energy which has a reported bond energy of 192 kJ/mol [15,21]. The measured bond enthalpy is in excellent agreement with a 2c-3e bonded interaction and also in accord with other experimental and computed 2c-3e sulfur–sulfur bonding interactions. The Se∴Se bond enthalpy and entropy of reaction are both lower than previously published S∴S interactions. The Se∴Se bond is approximately 15 kJ/mol weaker than S∴S interactions that average around 110 kJ/mol. This might be attributed to the larger atomic size of selenium relative to sulfur, resulting in a weaker bond. The entropy of reaction is about 30 J/mol K less negative than those found for the S∴S systems. A smaller entropy of reaction is expected for a more weakly bonded system because the more weakly bonded the products are, the more "reactant like" they may be. Hence, we expect a smaller entropy of reaction for more weakly bound association products. This argument however cannot lead to a quantitative result.

Experiments on the equilibrium reaction

$$(CH_3)_2Se^{\bullet +} + S(CH_3)_2 \rightleftharpoons [(CH_3)_2Se\therefore S(CH_3)_2]^+ \quad (2)$$

were attempted. However, we were unable to establish conditions which resulted in residence time distributions which were superimposable. Therefore, we were not able to establish thermodynamic equilibrium in our ion source. Equilibrium experiments on $[(CH_3)_2Se\therefore ICH_3]^+$ were not carried out since CH_3I gas reacts with $Se(CH_3)_2$ gas forming a trimethylselenononium iodide salt [22].

4. Conclusions

We believe the results presented here are the first gas-phase experiments on 2c-3e bonded systems involving selenium atoms. Our data support the structures: $[(CH_3)_2Se\therefore Se(CH_3)_2]^+$, $[(CH_3)_2Se\therefore S(CH_3)_2]^+$ and $[(CH_3)_2Se\therefore ICH_3]^+$. The metastable spectra of $[(CH_3)_2Se\therefore Se(CH_3)_2]^+$ and $[(CH_3)_2Se\therefore S(CH_3)_2]^+$ show only direct cleavage of the 2c-3e bond. However, $[(CH_3)_2Se\therefore ICH_3]^+$ shows direct cleavage and ejection of the iodine atom. The later path must involve a rearrangement and is not a

simple direct fragmentation reaction. The spectra of $[(CH_3)_2Se\therefore Se(CH_3)_2]^+$ were compared to those of $[CH_3Se–SeCH_3]^{\bullet+}$. Both the metastable and CID spectra of these two ions are different and very strongly support the conclusion that the former contains a 2c-3e Se∴Se bond while the latter contains a 2c-2e Se–Se bond. The CID spectra of all the Se-containing cations studied here show a remarkable propensity for $CH_3^\bullet$ loss; this is true of all methyl groups in the molecule whether bonded to Se, S or I. The propensity for $CH_3^\bullet$ loss may be due to the large "soft" nature of the selenium atom.

The thermodynamic equilibrium experiments resulted in what we believe is the first experimental 2c-3e bond enthalpy for a Se∴Se interaction. The value of $\Delta H^\circ_{bond} = 95$ kJ/mol is in intuitive agreement when compared to 2c-2e Se–Se bond energies as well as when compared to reported 2c-3e S∴S bond energies and enthalpies.

Acknowledgements

AJI is grateful to BASF (Germany) for donating the ZAB-1F to Auburn University and his research group in 1994 and to the Auburn University Chemistry Department for making this research possible. JEK acknowledges the Chemistry Department for a TA and the opportunity to further his education.

References

[1] L. Pauling, J. Am. Chem. Soc. 53 (1931) 3225.
[2] (a) A.J. Illies, P. Livant, M.L. McKee, J. Am. Chem. Soc. 110 (1988) 7980;
(b) Y. Deng, A.J. Illies, M.A. James, M.L. McKee, M. Peschke, J. Am. Chem. Soc. 117 (1995) 420;
(c) M.A. James, M.L. McKee, A.J. Illies, J. Am. Chem. Soc. 118 (1996) 7842.
[3] (a) A.J. Illies, L.S. Nichols, M.A. James, J.Am. Soc, Mass Specrtoscopy 8 (1997) 605;
(b) M.A. James, A.J. Illies, J. Phys. Chem. 100 (1996) 15794.
[4] S. Ekern, A.J. Illies, M.L. McKee, M. Peschke, J. Am. Chem. Soc. 115 (1993) 12510.
[5] M. Peschke, M.L. McKee, A.J. Illies, unpublished work on the ring expansion involving $[c\text{-}C_3H_6S\therefore S\ c\text{-}C_3H_6]^+$.
[6] A.J. Illies, J. Phys. Chem. 102 (1998) 8774.
[7] L.S. Nichols, A.J. Illies, J. Am. Chem. Soc. 121 (1999) 9176.
[8] (a) P. Livant, A.J. Illies, J. Am. Chem. Soc. 113 (1991) 1510;
(b) L.S. Nichols, M.L. McKee, A.J. Illies, J. Am. Chem. Soc. 120 (1998) 1538.
[9] L.S. Nichols, A.J. Illies, Int. J. Mass Spectrom. 185–187 (1999) 413.
[10] J.E. King, A.J. Illies, J. Phys. Chem. 106 (2002) 12248.
[11] (a) S.P. de Visser, L.J. de Koning, N.M.M. Nibbering, Int. J. Mass Spectrom. (120) (1998) 1517;
(b) S.P. de Visser, B.F. Matthias, L.J. de Koning, N.M.M. Nibbering, J. Am. Chem. Soc. 179/180 (1998) 43.
[12] J. A Booze, T. Baer, J. Chem. Phys. 96 (1992) 5541.
[13] (a) K.-D. Asmus, Nukleonika 45 (2000) 3;
(b) K.-D. Asmus, in: C. Chatgilialoglu, K.-D. Asmus (Eds.), Sulfur-Centered Reactive Intermediates in Chemistry and Biology, Plenum Press, New York, 1990, p. 155.
[14] K. Nishikida, F. Williams, Chem. Phys. Lett. 34 (1975) 302.
[15] (a) B. Braida, S. Hazebroucq, P.C. Hiberty, J. Am. Chem. Soc. 124 (2002) 2371;
(b) M. Maung, J.O. Williams, A.C. Wright, Theochemistry 453 (1988) 181;
(c) C. Glidewell, J. Organomet. Chem. 461 (1993) 15.
[16] (a) T.C. Stadtman, Annu. Rev. Biochem. 71 (2002) 1;
(b) N. Gupta, T.D. Porter, J. Biochem. Mol. Toxicol. 16 (2002) 18;
(c) L. Zhong, A. Holmgren, J. Biol. Chem. 275 (2000) 18121.
[17] (a) K.C. Thompson, C.E. Canosa-Mas, R.P. Wayne, Phys. Chem. Chem. Phys. 4 (2000) 4133;
(b) R. Atkinson, S.M. Aschmann, D. Hasegawa, E.T. Thompson-Eagle, W.T. Frankenberger Jr., Environ. Sci. Technol. 24 (1990) 1326.
[18] M.T. Bowers, A.J. Illies, M.F. Jarrold, Chem. Phys. 65 (1982) 19.
[19] A.J. Illies, T.H. Morton, Int. J. Mass Spectrom. Ion Processes 167/168 (1997) 431.
[20] Below 462 K the reactant ion intensity became vanishingly small. The ion source materials (Viton "O" rings and Teflon spacers) dictate the upper limit of 560 K.
[21] http://www.chem.ox.ac.uk/icl/dermot/nonmetalsold/lecture1/page11.html.
[22] Y. Imai, K. Aida, K. Itaya, Spectrochimica Acta 44A (1988) 179.